Journal of ELECTRONIC MATERIALS, Vol. 46, No. 2, 2017
DOI: 10.1007/s11664-016-4851-4
© 2016 The Minerals, Metals & Materials Society

CrossMark

Stability of Indium Gallium Zinc Aluminum Oxide Thin-Film Transistors with Treatment Processes

YUNG-HAO LIN[1] and CHING-TING LEE[1,2,3]

1.—Institute of Microelectronics, Department of Electrical Engineering, Research Center for Energy Technology and Strategy, National Cheng Kung University, Tainan 701, Taiwan, Republic of China. 2.—Da-Yeh University, Changhua 515, Taiwan, Republic of China. 3.—e-mail: ctlee@ee.ncku.edu.tw

The indium-gallium-zinc-aluminum-oxide (IGZAO) channel layer of the bottom-gate-type thin-film transistors (TFTs) was deposited on indium tin oxide-coated glass substrates using a magnetron radio frequency co-sputtering system with dual targets of indium gallium zinc oxide and Al. The 3 s orbital of Al cations provided an extra transport pathway and widened the bottom of the conduction band, thus increasing the electron mobility in the IGZAO films. The Al-O bonds could sustain the stability of oxygen of the IGZAO films. The IGZAO TFTs were processed by O_2 plasma and post-annealing treatments. Hysteresis analysis was carried out in order to study the stability of the resulting IGZAO TFTs, the positive bias temperature stress (PBTS) performance, and the hot carrier effect were also measured. For the IGZAO TFTs, the threshold voltage shift of the PBTS performance and the hot carrier effect were 0.1 V and 0.06 V, respectively. Overall, the IGZAO TFTs exhibited good stability in this study.

Key words: Indium-gallium-zinc-aluminum-oxide, magnetron radio frequency co-sputtering system, thin-film transistors

INTRODUCTION

Thin-film transistors (TFTs) are widely used as core components in electronic displays, especially in liquid crystal displays (LCD) and flexible electronics, among other applications.[1,2] The most commonly used materials for the channel layer of TFTs are amorphous silicon (a-Si)[3,4] and low temperature polycrystal silicon (LTPS).[5,6] However, the low energy bandgaps of these materials mean that they are susceptible to the influence of visible light, leading to the generation of photocurrent.[7] Moreover, there is a growing demand for displays with a high driving current and high electron mobility, and thus more attention has been paid to the use of indium-gallium-zinc-oxide (IGZO) TFTs, due to their higher transmittance and reasonably high electron mobility.[8,9] As such, IGZO is now being used as the channel layer of TFTs for active matrix organic light emitting diode (AMOLED) displays.[10,11] Advanced AMOLED displays have high pixel resolution and large frame size, and, thus, require high performance TFTs with a high mobility and low subthreshold swing. Furthermore, the issue of electrical reliability is critical with regard to high-current density conditions when oxide TFTs are applied in AMOLED displays.[12] IGZO TFTs suffer from electrical deterioration when operated under continued stress biases, due to the additional bias duration and magnitude.[13] In order to address such shortcomings, quinary indium gallium zinc aluminum oxide (IGZAO) films and IGZAO TFTs have been fabricated using a magnetron radio-frequency (RF) co-sputtering system with dual targets of IGZO and Al. The 3 s orbital of Al cations can provide extra transport pathways and widen the bottom of the conduction band, thus increasing the electron mobility in the IGZAO films. The Al-O bonds could also increase the stability of the oxygen in the IGZAO films.[14] However, in order to obtain more stable performance of IGZAO TFTs operated under

(Received April 22, 2016; accepted August 4, 2016; published online October 21, 2016)

high-current density conditions, the films are with O_2 plasma treatment[15] and post-annealing treatment. Therefore, IGZO TFTs and IGZAO TFTs undergoing these treatments were investigated in this work. The TFTs were passivated by a SiO_2 layer and systematically analyzed with regard to hysteresis, positive bias temperature stress (PBTS), and the hot carrier effect.

EXPERIMENTS

The IGZO films were deposited using an IGZO target with the atomic ratio (In:Ga:Zn = 3.52:1:2.72)[9] using a magnetron RF co-sputtering system. The RF power of the IGZO target was kept at 100 W. The IGZAO films were co-sputtered using the same IGZO target and the Al target (99.99%). The RF power of the Al target was 45 W, while the RF power of the IGZO target was kept at 100 W.[14] An Ar/O_2 gas flow rate of 60 sccm/40 sccm, and a chamber pressure of 0.01 kPa were used for depositing the IGZO and IGZAO films. Figure 1 shows the schematic configuration of the IGZAO TFTs. The structure of the bottom-gate-type TFTs was fabricated on the indium tin oxide (ITO)-coated glass substrate at room temperature using a magnetron RF co-sputtering system. The ITO gate was patterned by a standard photolithography and wet etched by the etching solution of $HCl:HNO_3$:Deionized water = 50:5:55. A 200-nm-thick SiO_2 film was then deposited as the gate insulator. The channel layers used the above-mentioned IGZO and IGZAO films, with 50-nm-thick IGZO and IGZAO channel layers deposited on the SiO_2 layer. The surfaces of the channel layers were revamped by the O_2 plasma treatment for 5 min. A 200-nm-thick Al layer was patterned and deposited as the source/drain electrodes. A 15-nm-thick SiO_2 passivated layer covered the resulting TFTs, and this was then subject to heat treatment at 300°C in air ambience for 10 min using a rapid thermal annealing system. The channel width and the channel length were 100 μm and 10 μm, respectively.

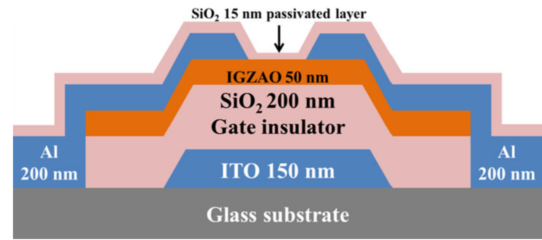

Fig. 1. Schematics configuration of the IGZAO TFTs.

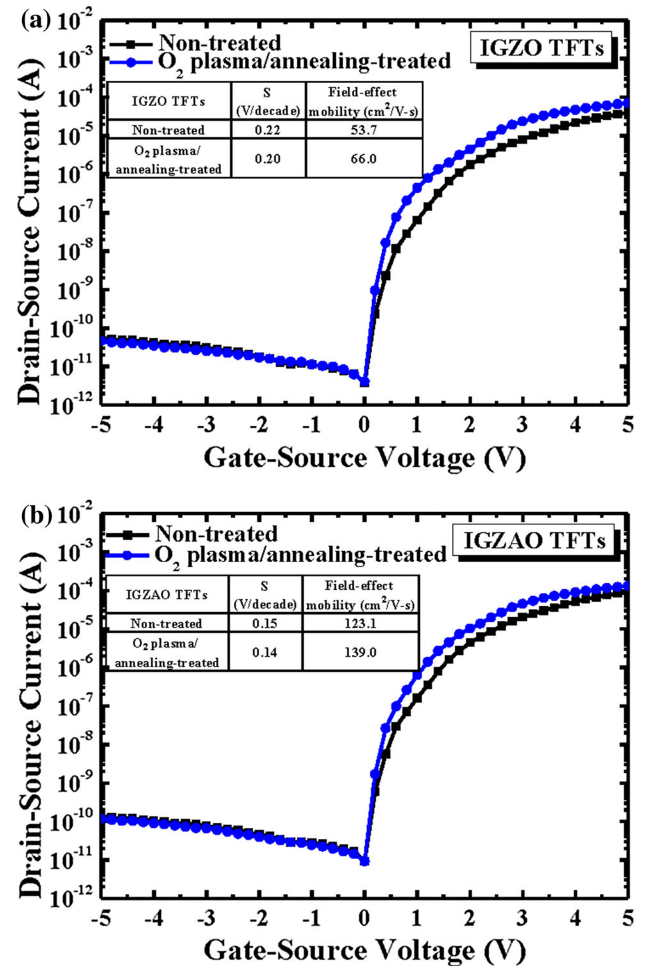

Fig. 2. Drain-source current–drain-source voltage transfer characteristics of (a) the IGZO TFTs and (b) the IGZAO TFTs after O_2 plasma treatment and post-annealing treatment.

EXPERIMENTAL RESULTS AND DISCUSSION

Figure 2a and b show the drain-source current–gate-source voltage (i_{DS}–v_{GS}) transfer characteristics of the IGZO TFTs and IGZAO TFTs after O_2 plasma treatment and post-annealing treatment, respectively. The drain-source current i_{DS} as a function of the drain-source voltage v_{DS} of the TFTs operating in the triode region can be described as[16]:

$$i_{DS} = \frac{W}{L}\mu_{FE}C_{OX}\left[(v_{GS} - V_T)v_{DS} - \frac{1}{2}v_{DS}^2\right], \quad (1)$$

where W and L are the channel width and channel length, respectively, μ_{FE} is the field-effect mobility, V_T is the threshold voltage, and C_{OX} is the capacitance per unit area. From the i_{DS}–v_{GS} transfer characteristics shown in Fig. 2, the transconductance g_m was obtained from the following equation:

$$g_m = \partial i_{DS}/\partial v_{GS}|_{v_{DS}=V_{DS}} = \frac{W}{L}\mu_{FE}C_{OX}V_{DS}. \quad (2)$$

The g_m of the IGZO TFTs was improved from 1.76×10^{-5} S to 2.16×10^{-5} S, and that of the IGZAO TFTs was improved from 4.03×10^{-5} S to 4.55×10^{-5} S. Consequently, the μ_{FE} of the IGZO

TFTs was improved from 53.7 cm^2/V-s to 66.0 cm^2/V-s, and that of the IGZAO TFTs was improved from 123.1 cm^2/V-s to 139.0 cm^2/V-s. The subthreshold swing S of the TFTs was determined by the following equation[17]:

$$S = \partial v_{\mathrm{GS}} / \partial \log i_{\mathrm{DS}} |_{v_{\mathrm{DS}}=V_{\mathrm{DS}}}. \quad (3)$$

The subthreshold swing S could be obtained from the i_{DS}–v_{GS} transfer characteristics, as plotted in Fig. 2. The subthreshold swing S of the IGZO TFTs was improved from 0.22 V/decade to 0.20 V/decade, and that of the IGZAO TFTs was improved from 0.15 V/decade to 0.14 V/decade. It was worth noting that the electrical characteristics of IGZAO TFTs saw less improvement than the IGZO TFTs, despite the O_2 plasma treatment and post-annealing treatment. This is attributed to the fact that the IGZAO films were more stable, as the Al-O bonds stabilized the oxygen and reduced the formation of oxygen vacancies.

Figure 3 shows the hysteresis comparisons of the IGZO and IGZAO TFTs with the O_2 plasma and post-annealing treatments. The ΔV is the voltage shift between the forward sweep from -5 V to 5 V and the reverse sweep from 5 V to -5 V at a i_{DS} of 10^{-9} A. The ΔV of the IGZO TFTs with the O_2 plasma and post-annealing treatments was 0.4 V. However, the IGZAO TFTs after both treatments had a ΔV of nearly 0 V. This indicates that the IGZAO films were of high quality with low vacancies due to the low electron trapping at the front interface between the gate insulator and channel. Moreover, the positive bias temperature stress (PBTS) performance is the crucial property of the IGZO TFTs. The PBTS behaviors of the IGZO and IGZAO TFTs with the O_2 plasma and post-annealing treatments under various stress times are show in Fig. 4a and b, respectively. The PBTS characteristics were measured by applying a v_{GS} stress bias of 20 V, under a stress temperature of 80°C. The threshold voltage V_{T} of the IGZO TFTs changed from 1.08 V to 1.56 V as the stress time increased from 0 s to 2000 s. The V_{T} change of the IGZAO TFTs was only 0.1 V, from 1.03 V to 1.13 V, as the stress time increased from 0 s to 2000 s. This is attributed to the fact that the traps' states in the channel layer, and at the interface between the gate insulator and the channel layer, were filled by the v_{GS} bias stress. However, the V_{T} changes indicated that the electric devices were influenced by the existence of trap states. It is noted that there were much fewer trap states in the IGZAO TFTs than in the IGZO TFTs, due to the high quality of IGZAO films and interface. The threshold shift of the IGZAO TFTs was 80% smaller than that of the IGZO TFTs. Therefore, the IGZAO TFTs exhibited stable PBTS performance due to the few trap states in the IGZAO TFTs.

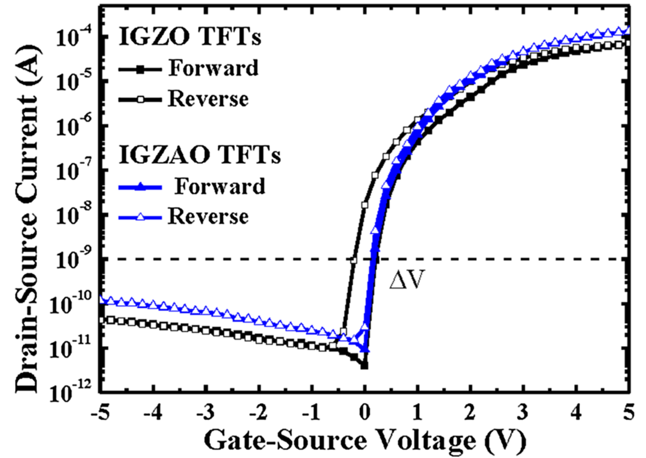

Fig. 3. Hysteresis comparisons of the IGZO TFTs and the IGZAO TFTs with the O_2 plasma and post-annealing treatments.

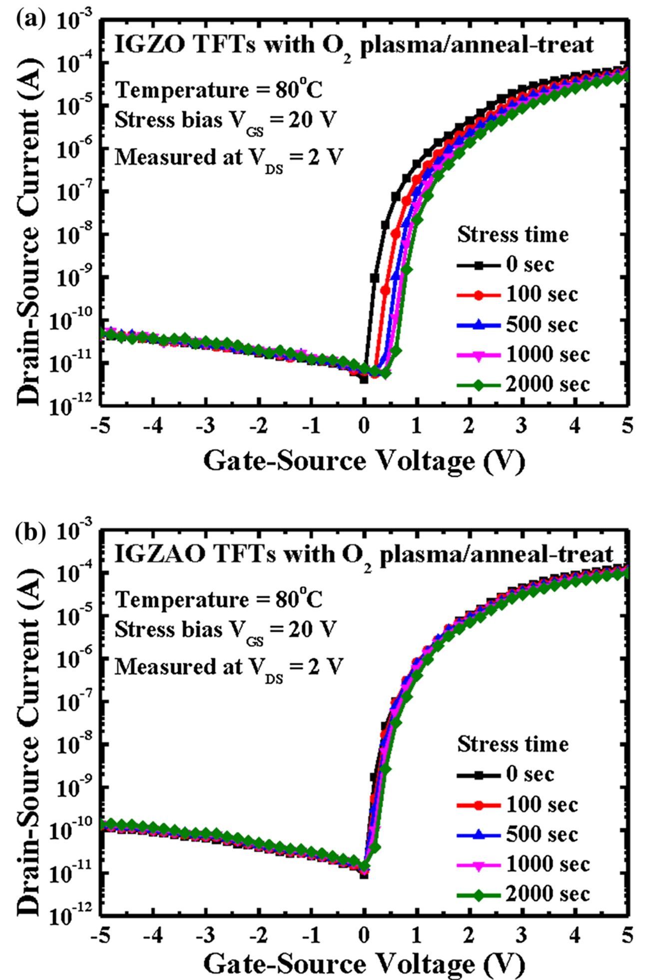

Fig. 4. PBTS behavior of (a) the IGZO TFTs and (b) the IGZAO TFTs with the O_2 plasma and post-annealing treatments under various stress times.

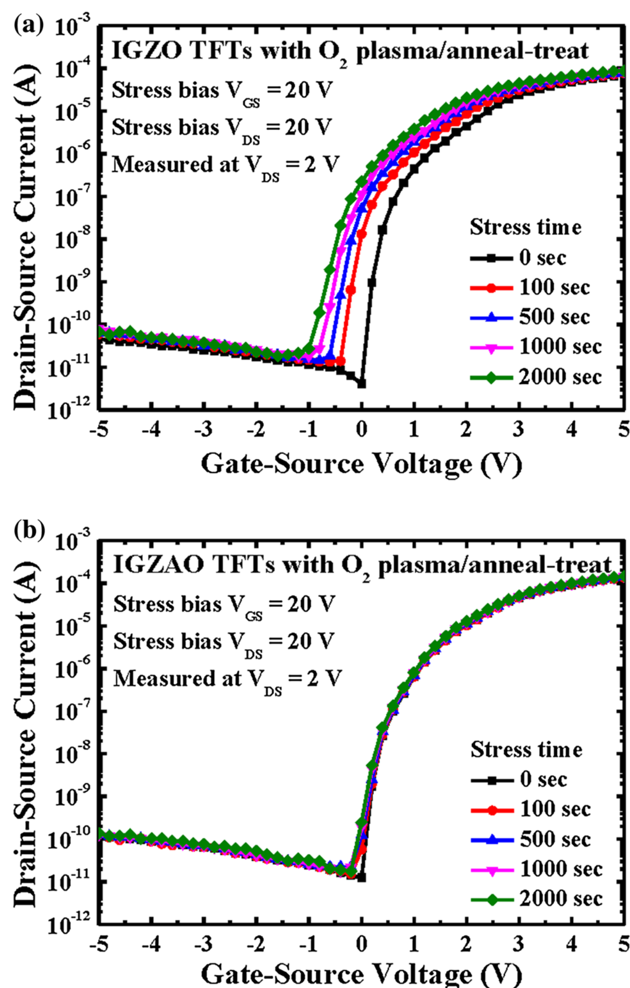

Fig. 5. Hot carrier effect of (a) the IGZO TFTs and (b) the IGZAO TFTs with various stress times, measured at v_{DS} = 2 V.

Thermal issues are a critical factor for silicon-on-insulator (SOI) TFTs on glass substrates.[18] The key phenomenon here is known as the hot carrier effect, which has negative impacts on the performance of IGZO TFTs. The hot carrier effect causes the operating temperature to rise and, thus, deteriorates the IGZO TFTs. To investigate the hot carrier effect, a v_{GS} and a v_{DS} of 20 V were simultaneously applied to the IGZO and IGZAO TFTs. The hot carrier effect performances of the IGZO and IGZAO TFTs for various stress times, measured at v_{DS} = 2 V, are shown in Fig. 5a and b. The threshold voltage of the IGZO TFTs shifted from 1.08 V to 0.12 V when the bias time was raised from 0 s to 2000 s. It is worth noting that the IGZO TFTs had an obviously negative threshold voltage shift, and this is attributed to the high lateral electric field induced by the high current density and the electron–hole pair generation that is caused by impact ionization. The holes created by impact ionization accumulate and are trapped at the interface between the channel and passivated layers, near the source junction. The trapped holes then reduce the electrical potential wall, and so increase electron injection.[19] Therefore, the drain-source current i_{DS} increased at the subthreshold region, and at the same time did the threshold voltage. The change in threshold voltage of the IGZAO TFTs was about 0.06 V, from 1.03 V to 0.97 V, as the bias time increased from 0 s to 2000 s. This result implies that the IGZAO TFTs had good stability performance due to the Al-O bonds in the IGZAO films, and, thus, the IGZAO TFTs had better interfaces, which reduced the hot carrier effect.

CONCLUSIONS

IGZAO films were deposited using dual targets of Al and IGZO by the magnetron RF sputtering system. The IGZAO films were stabilized by the strong Al-O bonds, and the IGZAO TFTs also exhibited high stability. Hysteresis analysis was carried out to investigate the stability of the IGZAO TFTs, and the PBTS performances and hot carrier effect were also measured. In the hysteresis analysis, the voltage shift ΔV of the IGZAO TFTs operated at the interval from −5 V to 5 V was less than 0.1 V. The PBTS performances were biased at a gate-source voltage of 20 V for 2000 s, and the threshold voltage shift of the IGZAO TFTs was only 0.1 V. In the hot carrier effect measurement, a gate-source voltage of 20 V and a drain-source voltage of 20 V were continually biased for 2000 s. The shift in threshold voltage of the IGZAO TFTs was about 0.06 V when the hot carrier effect was measured. The stability of the IGZAO TFTs was to the good oxygen stability due to the strong Al-O bonds in the IGZAO channel layer. The results of this study show that the IGZAO TFTs produced in this work are applicable for use in advanced display products.

ACKNOWLEDGEMENTS

This work was supported by the Research Center for Energy Technology and Strategy of National Cheng Kung University and the Ministry of Science and Technology of Republic of China under Contract No. MOST 105-2221-E-006-199-MY3.

REFERENCES

1. H.J. In and O.K. Kwon, *IEEE Electron Device Lett.* 33, 1018 (2012).
2. J.S. Park, T.W. Kim, D. Stryakhilev, J.S. Lee, S.G. An, Y.S. Pyo, D.B. Lee, Y.G. Mo, D.U. Jin, and H.K. Chung, *Appl. Phys. Lett.* 95, 013503 (2009).
3. H. Lee, G. Yoo, J.S. Yoo, and J. Kanicki, *J. Appl. Phys.* 105, 124522 (2009).
4. C.R. Wie, Z. Tang, and M.S. Park, *J. Appl. Phys.* 104, 114509 (2008).
5. T. Suzuki, *J. Appl. Phys.* 99, 111101 (2006).
6. K.M. Chang, B.W. Huang, C.H. Wu, I.-C. Deng, T.C. Chang, and S.C. Lin, *Solid State Electron.* 111, 7 (2015).
7. C.T. Lee and Y.H. Lin, *Appl. Phys. Express* 7, 076502 (2014).
8. M. Kim, J.H. Jeong, H.J. Lee, T.K. Ahn, H.S. Shin, J.S. Park, J.K. Jeong, Y.G. Mo, and H.D. Kim, *Appl. Phys. Lett.* 90, 212114 (2007).
9. C.T. Lee, Y.H. Lin, M.M. Chang, and H.Y. Lee, *IEEE J. Disp. Technol.* 10, 293 (2014).

10. S. Yang, C.S. Hwang, J.I. Lee, S.M. Yoon, M.K. Ryu, K.I. Cho, S.H.K. Park, S.H. Kim, C.E. Park, et al., *Appl. Phys. Lett.* 98, 103515 (2011).
11. S.I. Kim, S.W. Kim, C.J. Kim, and J.S. Park, *J. Electrochem. Soc.* 158, H115 (2011).
12. J.M. Lee, I.T. Cho, J.H. Lee, and H.I. Kwon, *Appl. Phys. Lett.* 93, 093504 (2008).
13. S. Hashimoto, Y. Uraoka, T. Fuyuki, and Y. Morita, *Jpn. J. Appl. Phys.* 46, 1387 (2007).
14. C.T. Lee, Y.H. Lin, and J.H. Lin, *J. Appl. Phys.* 117, 045309 (2015).
15. H.F. Pu, Q.F. Zhou, L. Yue, and Q. Zhang, *Appl. Surf. Sci.* 283, 722 (2013).
16. M. Shur, M. Hack, and J.G. Shaw, *J. Appl. Phys.* 66, 3371 (1989).
17. R. Martins, P. Barquinha, I. Ferreira, L. Pereira, G. Gonçalves, and E. Fortunato, *J. Appl. Phys.* 101, 044505 (2007).
18. K. Watanabe and T. Asano, *Jpn. J. Appl. Phys.* 48, 03B005 (2009).
19. S.H. Choi and M.K. Han, *Appl. Phys. Lett.* 100, 043503 (2012).